Control of an Unstable, Nonminimum Phase Hypersonic Vehicle Model

Michael W. Oppenheimer, Senior Member
David B. Doman, Member
Control Design and Analysis Branch
2210 Eighth St., Bldg. 146, Rm. 305
Wright-Patterson AFB, OH, USA
937-255-8490
michael.oppenheimer@wpafb.af.mil

Abstract— In this work, a control law for an unstable, nonminimum phase model of a hypersonic vehicle is developed. The control problem is difficult due to the locations of the plant poles and zeros. For an unstable system, feedback is required to stabilize the plant. However, one cannot make the loop gains arbitrarily large without driving one or more of the closed-loop poles into the right-half of the s-plane, since the system is nonminimum phase. Thus, there is a limited range of feedback gain that results in a stable system. The nonminimum phase behavior also places restrictions on the closed-loop bandwidth. For the hypersonic vehicle control problem, low frequency control is desired and a rule of thumb is that the closed-loop bandwidth must be less than one-half the right-half plane zero location. A right-half plane zero located in the region of the desired gain-crossover frequency makes it impossible to achieve the desired level of tracking performance. The achievable closed-loop bandwidth might be so small that adequate control of the system is not achieved. Direct cancellation of the right-half plane zero with an unstable pole in the controller is not an option. In this work, a modified dynamic inversion controller is developed for a linear, time-invariant model of a hypersonic vehicle. This modified dynamic inversion controller differs from the standard dynamic inversion approach in that it does not attempt to cancel the right-half plane zero with a pole, instead, it retains right-half plane zeros in the closed-loop transfer functions and uses an additional feedback loop to stabilize the zero dynamics.

TABLE OF CONTENTS

IEEEAC paper # 1409, Version 2, Updated Dec. 12, 2005

1. HSV MODEL

The model to be controlled in this case is given by

$$\begin{array}{c}\dot{\mathbf{x}} = \mathbf{Ax}+\mathbf{Bu} \\ \mathbf{y}=\mathbf{Cx}+\mathbf{Du}\end{array} \tag{1}$$

where $\mathbf{A} \in \mathbb{R}^{nxn}$, $\mathbf{B} \in \mathbb{R}^{nxm}$, $\mathbf{C} \in \mathbb{R}^{pxn}$, $\mathbf{D} \in \mathbb{R}^{pxm}$, and $n = 9$, $m = p = 2$. The model outputs are velocity (ft/sec) and flight path angle (deg), while the inputs are elevator deflection (deg) and temperature addition in the combustor (deg R). More specifically, the state-space matrices, derived from a nonlinear model [1], are

$$\mathbf{A} = \left[\begin{array}{cc} \mathbf{A}_1 & \mathbf{A}_2 \end{array}\right] \tag{2}$$

where

$$\mathbf{A}_1 = \left[\begin{array}{ccccc} -4.8e^{-4} & 2.05 & 0 & -5.1e^{-6} & -32.17 \\ -5.8e^{-7} & -.077 & 1 & 1.9e^{-7} & 0 \\ -1.29e^{-5} & .07 & 0 & 2.39e^{-6} & 0 \\ 0 & -7846.36 & 0 & 0 & 7846.36 \\ 0 & 0 & 1 & 0 & 0 \\ 0 & 0 & 0 & 0 & 0 \\ -.068 & -7368.3 & 0 & .0159 & 0 \\ 0 & 0 & 0 & 0 & 0 \\ -.076 & -5668.22 & 0 & .018 & 0 \end{array}\right] \tag{3}$$

$$\mathbf{A}_2 = \left[\begin{array}{cccc} .084 & 0 & -.513 & 0 \\ -9.69e^{-5} & 0 & -1.59e^{-4} & 0 \\ -.028 & -8.77e^{-5} & -.01 & -7.73e^{-6} \\ 0 & 0 & 0 & 0 \\ 0 & 0 & 0 & 0 \\ 0 & 1 & 0 & 0 \\ -286.5 & -.641 & 1.518 & 1.078e^{-3} \\ 0 & 0 & 0 & 1 \\ -4.72 & 8.82e^{-4} & -401.39 & -.78 \end{array}\right] \tag{4}$$

$$\mathbf{B} = \left[\begin{array}{cc} -62.589 & 0.0064 \\ -.0222 & -2.61e^{-7} \\ -0.997 & 8.25e^{-7} \\ 0 & 0 \\ 0 & 0 \\ 0 & 0 \\ 139.032 & -.000115 \\ 0 & 0 \\ -2500.6 & -.0769 \end{array}\right] \tag{5}$$

$$\mathbf{C} = \begin{bmatrix} 1 & 0 & 0 & 0 & 0 & 0 & 0 & 0 & 0 \\ 0 & -1 & 0 & 0 & 1 & 0 & 0 & 0 & 0 \end{bmatrix} \tag{6}$$

$$\mathbf{D} = \begin{bmatrix} 0 & 0 \\ 0 & 0 \end{bmatrix} \tag{7}$$

The state vector is

$$\mathbf{x} = \begin{bmatrix} V & \alpha & Q & h & \theta & \eta_f & \dot{\eta}_f & \eta_a & \dot{\eta}_a \end{bmatrix}^T \tag{8}$$

where V denotes velocity or true airspeed, α denotes the angle of attack, q denotes the pitch rate, h is the altitude, θ is the pitch attitude, and the last four states represent temporal modal coordinates that describe the first bending mode of the fore and aft fuselage. The outputs of the model that we wish to control are the velocity V and the flight path angle $\gamma = \theta - \alpha$. The idea in this work is to use a dynamic inversion type scheme to control the plant and provide a desired response. Unfortunately, this plant is nonminimum phase, with poles and transmission zeros at the following locations:

$$Poles = \left\{ \begin{array}{c} -0.39 \pm j20.03 \\ -0.32 \pm j16.94 \\ -1.0035 \\ 0.9322 \\ -5.6e^{-4} \\ -3.88 \pm j0.041 \end{array} \right\} \tag{9}$$

$$Zeros = \left\{ \begin{array}{c} 0 \\ 1.949 \\ -1.948 \\ -0.391 \pm j19.58 \\ -0.321 \pm j16.95 \end{array} \right\} \tag{10}$$

Hence, dynamic inversion [2] (DI) is not an option due to the right-half plane zero. This is because DI will try to cancel plant zeros, thus resulting in a right-half plane pole in the closed-loop system. Fortunately, a DI type scheme can be used to circumvent this issue. Dynamic extension [3] retains the nonminimum phase zero (does not try to cancel it with an unstable pole), yet still has the desirable trait of decoupling the system. The following describes the development of a dynamic extension algorithm for the system described above.

2. Dynamic Extension

Consider the system described in Eq. 1. The vector $\mathbf{y}$ is a set of controlled variables (CVs). Dynamic inversion is used to decouple the system and produce desired responses from the CVs. To begin the development of the controller, consider each CV:

$$y_i = \mathbf{C}_i\mathbf{x} + \mathbf{D}_i\mathbf{u}, i = 1, 2 \tag{11}$$

Since each $\mathbf{D}_i$, $i = 1, 2$ is a row of zeros (see Eq. 7), the input does not explicitly show in the output equation. To obtain an equation with the input, differentiate y to obtain

$$\dot{y}_i = \mathbf{C}_i\dot{x} = \mathbf{C}_i\mathbf{A}\mathbf{x} + \mathbf{C}_i\mathbf{B}\mathbf{u} \tag{12}$$

In this case, $\mathbf{C}_i\mathbf{B} \neq \mathbf{0}$, $i = 1, 2$, so there is no need to take any more derivatives of the output. Now, the system dynamics are given by

$$\begin{aligned} \dot{\mathbf{x}} &= \mathbf{Ax}+\mathbf{Bu} \\ \dot{\mathbf{y}} &= \mathbf{CAx}+\mathbf{CBu} \end{aligned} \tag{13}$$

In order to decouple the controlled variables, the matrix **CB** must be right invertible. If this is the case, then

$$\mathbf{u} = (\mathbf{CB})^{-1}(\dot{\mathbf{y}}_{des} - \mathbf{CAx}) \tag{14}$$

where $\dot{\mathbf{y}}_{des}$ is a vector of pseudo-controls. In this case,

$$\dot{\mathbf{y}}_{des} = \begin{bmatrix} \dot{V}_{tdes} \\ \dot{\gamma}_{des} \end{bmatrix} \tag{15}$$

where V_t is the vehicle's velocity and γ is the flight path angle. Applying the vector u in Eq. 14 to the output and state dynamics equations produces

$$\begin{aligned} \dot{\mathbf{y}} &= \mathbf{CAx}+\mathbf{CBu} = \mathbf{CAx} + (\mathbf{CB})\left(\mathbf{CB}^{-1}\right)(\dot{\mathbf{y}}_{des} - \mathbf{CAx}) \\ &= \dot{\mathbf{y}}_{des} \end{aligned} \tag{16}$$

so that the controlled variables follow exactly the pseudo-controls and

$$\begin{aligned} \dot{\mathbf{x}} &= \mathbf{Ax}+\mathbf{Bu} = \mathbf{Ax} + \mathbf{B}\left(\mathbf{CB}^{-1}\right)(\dot{\mathbf{y}}_{des} - \mathbf{CAx}) \\ &= \left(\mathbf{A} - \mathbf{B}(\mathbf{CB})^{-1}\mathbf{CA}\right)\mathbf{x} + \mathbf{B}\left(\mathbf{CB}^{-1}\right)\dot{\mathbf{y}}_{des} \\ &= \mathbf{A}^x\mathbf{x} + \mathbf{B}\left(\mathbf{CB}^{-1}\right)\dot{\mathbf{y}}_{des} \end{aligned} \tag{17}$$

where

$$\mathbf{A}^x = \mathbf{A} - \mathbf{B}(\mathbf{CB})^{-1}\mathbf{CA} \tag{18}$$

As it turns out, the eigenvalues of $\mathbf{A}^x$ are the poles of the zero dynamics and are identically equal to the zeros of the original system (see Eq. 10). So, the state dynamics are determined by the inverse state space system

$$\begin{aligned} \dot{\mathbf{x}} &= \mathbf{A}^x\mathbf{x} + \mathbf{B}\left(\mathbf{CB}^{-1}\right)\mathbf{v} \\ \mathbf{x} &= \mathbf{Ix}+\mathbf{0v} \end{aligned} \tag{19}$$

Let **S** be a matrix of left eigenvectors of $\mathbf{A}^x$. Then, Eq. 19 can be transformed into the following Jordan form

$$\dot{\boldsymbol{\xi}} = \boldsymbol{\Lambda\xi} + \mathbf{SB}\left(\mathbf{CB}^{-1}\right)\mathbf{v} \tag{20}$$

where $\boldsymbol{\Lambda} = \mathbf{SA}^x\mathbf{S}^{-1}$. The states in Eq. 20 are related to the original states through the transformation $\boldsymbol{\xi} = \mathbf{Sx}$.

The transmission zeros, of a linear system with realization $\{\mathbf{A}, \mathbf{B}, \mathbf{C}\}$, are defined as the values of $\boldsymbol{\zeta}$, the vectors $\mathbf{z}_I, \mathbf{w}_I$, the input zero directions or $\mathbf{z}_O, \mathbf{w}_O$, the output zero directions that satisfy

$$\begin{bmatrix} (\boldsymbol{\zeta}\mathbf{I} - \mathbf{A}) & -\mathbf{B} \\ \mathbf{CA} & \mathbf{CB} \end{bmatrix} \begin{bmatrix} \mathbf{z}_I \\ \mathbf{w}_I \end{bmatrix} = \mathbf{0} \tag{21}$$

or

$$\begin{bmatrix} \mathbf{z}_O & \mathbf{w}_O \end{bmatrix} \begin{bmatrix} (\boldsymbol{\zeta}\mathbf{I} - \mathbf{A}) & -\mathbf{B} \\ \mathbf{CA} & \mathbf{CB} \end{bmatrix} = \mathbf{0} \tag{22}$$

From the output zero case, solve for $\mathbf{z}_0$ to get

$$-\mathbf{z}_0\mathbf{B} + \mathbf{w}_0\left(\mathbf{CB}^{-1}\right) = 0 \tag{23}$$

Solving for $\mathbf{w}_0$ yields

$$\mathbf{w}_0 = \mathbf{z}_0\mathbf{B}\left(\mathbf{CB}^{-1}\right) \tag{24}$$

Substituting Eq. 24 into the first output equation in Eq. 22 yields

$$\begin{aligned}\mathbf{z}_0\left(\boldsymbol{\zeta}\mathbf{I} - \mathbf{A}\right) + \mathbf{w}_0\mathbf{CA} &= \mathbf{z}_0\left(\boldsymbol{\zeta}\mathbf{I} - \mathbf{A} + \mathbf{B}\left(\mathbf{CB}^{-1}\right)\mathbf{CA}\right) \\ &= \mathbf{0}\end{aligned} \tag{25}$$

Hence, the transmission zeros are the eigenvalues of the matrix $\left(\mathbf{A} - \mathbf{B}\left(\mathbf{CB}^{-1}\right)\mathbf{CA}\right)$, which is identically equal to the matrix $\mathbf{A}^x$ defined in Eq. 18. This result shows that the transmission zeros of the original system are poles of the zero dynamics of the dynamic inversion. Thus, if the original system is nonminimum phase, then applying standard dynamic inversion will result in zero dynamics with right half plane poles. In order to obtain stable zero dynamics, the desired dynamics of the CVs must be modified. This requirement is due to the nonminimum phase behavior of the original system. Additionally, the vectors $\mathbf{z}_0$ are the eigenvectors of $\mathbf{A}^x$. Gathering all these eigenvectors into a matrix, $\mathbf{Z}_0$, it is seen that $\mathbf{Z}_0$ is a matrix of left eigenvectors of $\mathbf{A}^x$. Hence, $\mathbf{Z}_0 = \mathbf{S}$. Then, from Eq. 24,

$$\mathbf{W}_0 = \mathbf{Z}_0\mathbf{B}\left(\mathbf{CB}^{-1}\right) = \mathbf{SB}\left(\mathbf{CB}^{-1}\right) \tag{26}$$

3. Modified Dynamic Inversion Controller

Case 1

Suppose that one transmission zero, ζ_i, is in the right-half plane and would thus result in unstable zero dynamics. Without loss of generality, suppose that the output zero direction is given by

$$\mathbf{w}_0^{RHP} = \left[\begin{array}{cc} 0 & w_0^{RHP}{}_2 \end{array}\right] \tag{27}$$

This means that only pseudo-input 2 excites the unstable zero state (the state corresponding to the nonminimum phase zero). Hence, select $\dot{y}_{des2}$ to include a stabilizing term, from the unstable zero state (ξ^{RHP}), such that

$$v_2 = \dot{\gamma}_{des} + k_i\xi^{RHP} \tag{28}$$

In Jordan form, the dynamics of the unstable zero state become

$$\begin{aligned}\dot{\xi}^{RHP} &= \zeta_i\xi^{RHP} + \mathbf{w}_0^{RHP}\left[\begin{array}{c} v_1 \\ v_2 \end{array}\right] \\ &= \zeta_i\xi^{RHP} + 0v_1 + w_0^{RHP}{}_2 v_2 \\ &= \zeta_i\xi^{RHP} + w_0^{RHP}{}_2\left(\dot{\gamma}_{des} + k_i\xi^{RHP}\right)\end{aligned} \tag{29}$$

Thus,

$$\xi^{RHP} = \frac{w_0^{RHP}{}_2\dot{\gamma}_{des}}{s - \left(\zeta_i + w_0^{RHP}{}_2 k_i\right)} \tag{30}$$

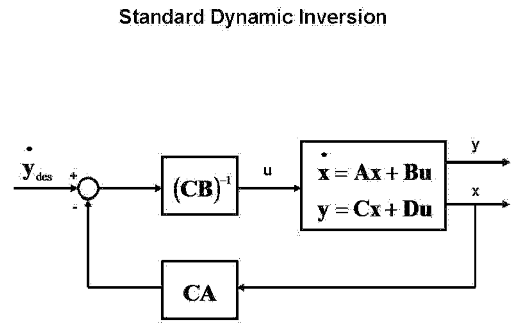

Figure 1. Standard Dynamic Inversion.

Note that k_i is selected so that $(\zeta_i + w_{0i12}k_i) < 0$. Substituting this result into Eq. 28, the new pseudo-control becomes

$$\begin{aligned}v_2 &= \dot{\gamma}_{des} + k_i\frac{w_0^{RHP}{}_2\dot{\gamma}_{des}}{s - \left(\zeta_i + w_0^{RHP}{}_2 k_i\right)} \\ &= \frac{s - \zeta_i}{s - \left(\zeta_i + w_0^{RHP}{}_2 k_i\right)}\dot{\gamma}_{des}\end{aligned} \tag{31}$$

With perfect inversion, $v_1 = \dot{V}_t$ and $v_2 = \dot{\gamma}$. Thus,

$$\begin{aligned}\left[\begin{array}{c} V_t \\ \gamma \end{array}\right] &= \left[\begin{array}{c} \frac{1}{s}\dot{V}_t \\ \frac{1}{s}\dot{\gamma} \end{array}\right] \\ &= \left[\begin{array}{cc} \frac{1}{s} & 0 \\ 0 & \frac{1}{s}\frac{s-\zeta_i}{s-\left(\zeta_i + w_0^{RHP}{}_2 k_i\right)} \end{array}\right]\left[\begin{array}{c} \dot{V}_{t_{des}} \\ \dot{\gamma}_{des} \end{array}\right]\end{aligned} \tag{32}$$

So, as desired, the system is now decoupled, however, the right-half plane zero is still present. This is unavoidable for a nonminimum phase plant. Figure 1 shows a standard dynamic inversion controller, while Figure 2 shows the modifications necessary to implement the modified dynamic inversion control law. Note that both Figures 1 and 2 are drawn assuming that the $\mathbf{D}$ matrix in Eq. 1 is identically zero and that the matrix $\mathbf{CB}$, Eq. 12, is nonzero and invertible. A slight modification must be made if these conditions are not met.

Case 2

Again, suppose that one transmission zero, ζ_i, is in the right-half plane and would thus result in unstable zero dynamics. Now, let the output zero direction be given by

$$\mathbf{w}_0^{RHP} = \left[\begin{array}{ccc} w_0^{RHP}{}_1 & w_0^{RHP}{}_2 \cdots w_0^{RHP}{}_p \end{array}\right] \tag{33}$$

In this case, multiple pseudo-inputs excite the bad zero state (the state corresponding to the nonminimum phase zero). In order to stabilize the system, select one pseudo-input to stabilize the state associated with the right-half plane zero (ξ^{RHP}). Hence, let

$$v_i = \dot{y}_{des_i} + k_i\xi^{RHP} \tag{34}$$

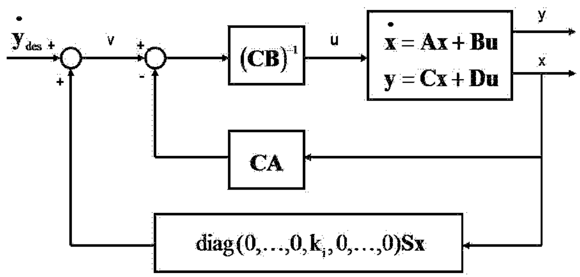

Figure 2. Modified Dynamic Inversion.

Then, from the form of $\mathbf{w}_0^{RHP}$ given in Eq. 33, the dynamics of the bad zero state become

$$\begin{aligned}\dot{\xi}^{RHP} &= \zeta_i \xi^{RHP} + \mathbf{w}_0^{RHP} \begin{bmatrix} v_1 \\ v_2 \\ \vdots \\ v_p \end{bmatrix} \\ &= \zeta_i \xi^{RHP} + w_0^{RHP}{}_1 v_1 + w_0^{RHP}{}_2 v_2 + \cdots + w_0^{RHP}{}_p v_p \\ &= \zeta_i \xi^{RHP} + w_0^{RHP}{}_1 v_1 \cdots + w_0^{RHP}{}_{i-1} v_{i-1} + w_0^{RHP}{}_i \\ &* \left(\dot{y}_{des_i} + k_i \xi^{RHP}\right) + w_0^{RHP}{}_{i+1} v_{i+1} + \cdots + w_0^{RHP}{}_p v_p \end{aligned} \tag{35}$$

Solving for ξ^{RHP} yields

$$\xi^{RHP} = \frac{p_1 + p_2 + w_0^{RHP}{}_i \dot{y}_{des_i}}{s - \left(\zeta_i + w_0^{RHP}{}_i k_i\right)} \tag{36}$$

where $p_1 = w_0^{RHP}{}_1 v_1 + \cdots + w_0^{RHP}{}_{i-1} v_{i-1}$ and $p_2 = w_0^{RHP}{}_{i+1} v_{i+1} + \cdots + w_0^{RHP}{}_p v_p$. Substituting Eq. 36 into Eq. 34 and simplifying yields

$$v_i = \frac{(s - \zeta_i)\, \dot{y}_{des_i}}{s - \left(\zeta_i + w_0^{RHP}{}_i k_i\right)} + k_i \left(\frac{p_1 + p_2}{s - \left(\zeta_i + w_0^{RHP}{}_i k_i\right)} \right) \tag{37}$$

Thus, exact decoupling is not achieved. In order to achieve decoupling, it is necessary to add another term to cancel the effects of $v_k, k = 1, 2, \cdots, p : k \neq p$. Hence, modify Eq. 34 to the following:

$$v_i = \dot{y}_{des_i} + k_i \xi^{RHP} + \sum_{j, j \neq i} \frac{q_{ij} \dot{y}_{des_j}}{s + \zeta_i} \tag{38}$$

Substituting Eq. 38 into Eq. 35 produces

$$\begin{aligned}\dot{\xi}^{RHP} &= \zeta_i \xi^{RHP} + \mathbf{w}_0^{RHP} \begin{bmatrix} v_1 \\ v_2 \\ \vdots \\ v_p \end{bmatrix} \\ &= \zeta_i \xi^{RHP} + w_0^{RHP}{}_1 v_1 + w_0^{RHP}{}_2 v_2 + \cdots + w_0^{RHP}{}_p v_p \\ &= \zeta_i \xi^{RHP} + w_0^{RHP}{}_1 v_1 + \cdots + w_0^{RHP}{}_{i-1} v_{i-1} + \\ & w_0^{RHP}{}_i \left(\dot{y}_{des_i} + k_i \xi^{RHP} + \sum_{j, j \neq i} \frac{q_{ij} \dot{y}_{des_j}}{s + \zeta_i} \right) + \\ & w_0^{RHP}{}_{i+1} v_{i+1} + \cdots + w_0^{RHP}{}_p v_p \end{aligned} \tag{39}$$

Solving for ξ^{RHP} in Eq. 39 and substituting this result into Eq. 38 gives

$$\begin{aligned} v_i &= \dot{y}_{des_i} + \\ k_i & \left[\frac{w_0^{RHP}{}_i \dot{y}_{des_i} + \sum_{j, j \neq i} \left(v_j w_0^{RHP}{}_j + w_0^{RHP}{}_i \frac{q_{ij} \dot{y}_{des_j}}{s + \zeta_i} \right)}{s - \left(\zeta_i + w_0^{RHP}{}_i k_i\right)} \right] \\ &+ \sum_{j, j \neq i} \frac{q_{ij} \dot{y}_{des_j}}{s + \zeta_i} \end{aligned} \tag{40}$$

Grouping like terms and simplifying Eq. 40 gives

$$\begin{aligned} v_i &= \frac{(s - \zeta_i)\, \dot{y}_{des_i}}{s - \left(\zeta_i + w_0^{RHP}{}_i k_i\right)} \\ &+ \frac{\sum_{j, j \neq i} \left(k_i v_j w_0^{RHP}{}_j + \frac{s - \zeta_i}{s + \zeta_i} q_{ij} \dot{y}_{des_j} \right)}{s - \left(\zeta_i + w_0^{RHP}{}_i k_i\right)} \end{aligned} \tag{41}$$

For complete decoupling, the second set of terms in Eq. 41 must be identically zero. Using this constraint and solving for v_j gives

$$v_j = \frac{-(s - \zeta_i)\, q_{ij} \dot{y}_{des_j}}{(s + \zeta_i)\, k_i w_0^{RHP}{}_i} \tag{42}$$

Letting

$$q_{ij} = k_i w_0^{RHP}{}_i \tag{43}$$

produces

$$v_j = \frac{-(s - \zeta_i)\, \dot{y}_{des_j}}{(s + \zeta_i)} \tag{44}$$

As before, with perfect inversion, $v_1 = \dot{V}_t$ and $v_2 = \dot{\gamma}$. Then, in this case, the expression between the desired and actual controlled variables becomes (Eq. 45)

So, as desired, the system is now decoupled, however, the right-half plane zero is still present. This is the penalty for a nonminimum phase plant.

$$
\begin{bmatrix} v_1 \\ v_2 \\ \vdots \\ v_i \\ \vdots \\ v_p \end{bmatrix} = \begin{bmatrix} \frac{-(s-\zeta_i)}{(s+\zeta_i)} & 0 & 0 & \cdots & 0 & \cdots & 0 \\ 0 & \frac{-(s-\zeta_i)}{(s+\zeta_i)} & 0 & 0 & 0 & \cdots & 0 \\ \vdots & \vdots & \vdots & \vdots & \vdots & \vdots & \vdots \\ 0 & \cdots & 0 & \frac{s-\zeta_i}{s-\left(\zeta_i+w_0^{RHP}{}_i k_i\right)} & 0 & \cdots & 0 \\ 0 & 0 & 0 & 0 & \cdots & 0 & \frac{-(s-\zeta_i)}{(s+\zeta_i)} \end{bmatrix} \begin{bmatrix} \dot{y}_{des_1} \\ \dot{y}_{des_2} \\ \vdots \\ \dot{y}_{des_i} \\ \vdots \\ \dot{y}_{des_p} \end{bmatrix} \tag{45}
$$

4. RESULTS

For the system described by Eqs. 1- 7, one zero is located in the RHP (see Eq. 10). In this case, $\mathbf{w}_0$ associated with the nonminimum phase zero is

$$
\mathbf{w}_{0i} = \begin{bmatrix} -0.000844 & 18.866 \end{bmatrix} \tag{46}
$$

For an initial design, assume that

$$
\mathbf{w}_{0i} = \begin{bmatrix} 0 & 18.866 \end{bmatrix} \approx \begin{bmatrix} 0 & 18.866 \end{bmatrix} \tag{47}
$$

so that case 1 applies. Thus, it can be seen that only the pseudo-input associated with the flight path angle, γ, affects the bad zero state. Let

$$
\begin{aligned} v_1 &= \dot{y}_{des_1} = \dot{V}_{tdes} \\ v_2 &= \dot{y}_{des_2} + k\xi^{RHP} = \dot{\gamma}_{des} + k\xi^{des} \end{aligned} \tag{48}
$$

Then,

$$
\begin{aligned} \dot{\xi}^{RHP} &= \lambda^{RHP}\xi^{RHP} + 18.866 v_2 \\ &= \lambda^{RHP}\xi^{RHP} + 18.866\left(\dot{\gamma}_{des} + k\xi^{RHP}\right) \end{aligned} \tag{49}
$$

Solving for ξ^{RHP} yields

$$
\xi^{RHP} = \frac{18.866}{s-(1.949+18.866k)}\dot{\gamma}_{des} \tag{50}
$$

and

$$
\begin{aligned} v_2 &= \dot{\gamma}_{des} + k\xi^{RHP} \\ &= \dot{\gamma}_{des} + k\left(\frac{18.866}{s-\{1.949+18.866k\}}\right)\dot{\gamma}_{des} \\ &= \left(\frac{s-1.949}{s-\{1.949+18.866k\}}\right)\dot{\gamma}_{des} \end{aligned} \tag{51}
$$

Selecting k in Eq. 52 to yield an all-pass filter, $k \approx -0.20667$ yields

$$
v_2 = \left(\frac{s-1.949}{s+1.949}\right)\dot{\gamma}_{des} \tag{52}
$$

Note that a right-half plane zero has two effects on the system, the first a magnitude and the second a phase. Unfortunately, the phase effects cannot be altered with this technique, however, the magnitude effects can be eliminated by choosing k so that an all-pass filter is obtained. Thus, the pole has been placed at the mirror (about the $j\omega$ axis) location in the left-half of the s-plane. Now, the pseudo-input relationship becomes

$$
\mathbf{v} = \begin{bmatrix} v_1 \\ v_2 \end{bmatrix} = \begin{bmatrix} 1 & 0 \\ 0 & \frac{s-1.949}{s+1.949} \end{bmatrix} \begin{bmatrix} \dot{V}_{tdes} \\ \dot{\gamma}_{des} \end{bmatrix} \tag{53}
$$

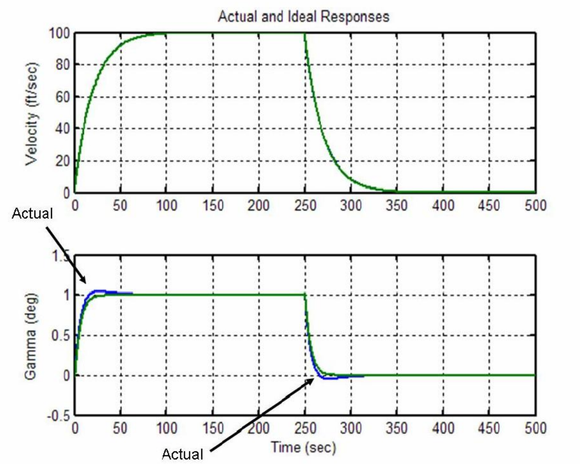

Figure 3. Velocity and Flight Path Angle vs. Time - Case 1.

With perfect inversion, the following closed-loop system is obtained

$$
\mathbf{v} = \begin{bmatrix} V_t \\ \gamma \end{bmatrix} = \begin{bmatrix} \frac{1}{s} & 0 \\ 0 & \frac{s-1.949}{s(s+1.949)} \end{bmatrix} \begin{bmatrix} \dot{V}_{tdes} \\ \dot{\gamma}_{des} \end{bmatrix} \tag{54}
$$

Figures 3 and 4 show the velocity and flight path angle responses along with the ideal response found using Eq. 54 and the control deflection time histories. A small amount of error exists and this is directly related to the assumption in Eq. 47.

It should be pointed out that prefilters were wrapped around the inversion controller. For the velocity channel, a simple proportional-integral prefilter was used, while for the flight path angle channel, a proportional-integral-derivative prefilter was used. The prefilters were the same for the simulation runs of cases 1 and 2.

Now, relax the assumption in Eq. 47 so that case 2 applies. Using Eqs. 42, 43, and 44 and selecting v_2 to stabilize the bad zero state yields

$$
v_2 = \dot{y}_{des_2} + k\xi^{RHP} = \dot{\lambda}_{des} + k\xi^{RHP} + \frac{q_{21}\dot{V}_{tdes}}{s+\lambda^{RHP}} \tag{55}
$$

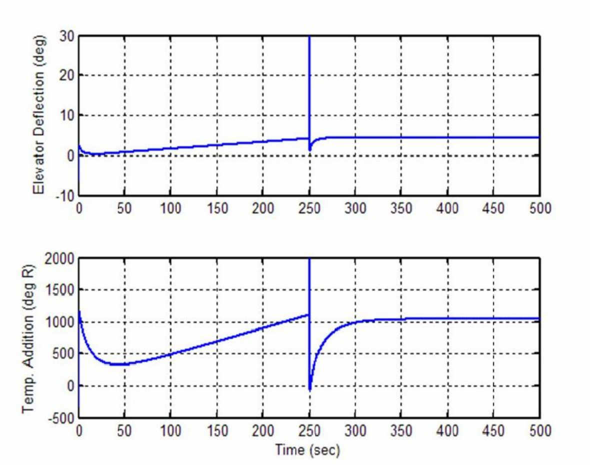

Figure 4. Control Deflections vs. Time - Case 1.

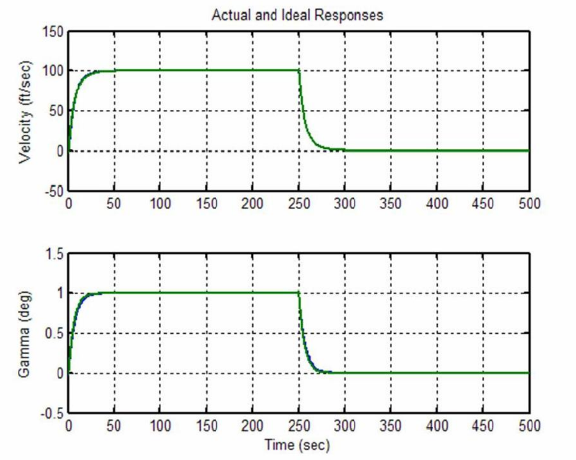

Figure 5. Velocity and Flight Path Angle vs. Time - Case 2.

Selecting $q_{21} = k w_0^{RHP}{}_1$ gives

$$\begin{aligned} v_1 &= \frac{s-\lambda^{RHP}}{s+\lambda^{RHP}} \dot{V}_{tdes} \\ v_2 &= \frac{s-\lambda^{RHP}}{s-\left(\lambda^{RHP}+w_0^{RHP}{}_2 k\right)} \dot{\gamma}_{des} \end{aligned} \tag{56}$$

Now, the pseudo-input relationship becomes

$$\begin{aligned} \mathbf{v} &= \begin{bmatrix} v_1 \\ v_2 \end{bmatrix} \\ &= \begin{bmatrix} \frac{s-\lambda^{RHP}}{s+\lambda^{RHP}} & 0 \\ 0 & \frac{s-\lambda^{RHP}}{s-\left(\lambda^{RHP}+w_0^{RHP}{}_2\right)} \end{bmatrix} \begin{bmatrix} \dot{V}_{tdes} \\ \dot{\gamma}_{des} \end{bmatrix} \end{aligned} \tag{57}$$

With perfect inversion, the following closed-loop system is obtained

$$\begin{aligned} \mathbf{y} &= \begin{bmatrix} V_t \\ \gamma \end{bmatrix} \\ &= \begin{bmatrix} \frac{1}{s}\left(\frac{s-\lambda^{RHP}}{s+\lambda^{RHP}}\right) & 0 \\ 0 & \frac{1}{s}\left(\frac{s-\lambda^{RHP}}{s-\left\{\lambda^{RHP}+w_0^{RHP}{}_2\right\}}\right) \end{bmatrix} \begin{bmatrix} \dot{V}_{tdes} \\ \dot{\gamma}_{des} \end{bmatrix} \end{aligned} \tag{58}$$

Figures 5 and 6 shows the velocity and flight path angle responses along with the ideal response found using Eq. 58. Notice that the error between the actual and ideal responses is much less than that seen in Fig. 4. Again, this is directly attributable to utilizing the case 2 work.

5. Conclusions

In this work, a dynamic inversion type controller was developed for an unstable, nonminimum phase hypersonic vehicle model. The technique used here allows decoupling of the system, in the same way that standard dynamic inversion allows decoupling. The difference is that the nonminimum phase zero cannot be cancelled by an unstable pole. Hence, the nonminimum phase zero is retained in the closed loop and a user selected gain is used to place the left-half plane pole.

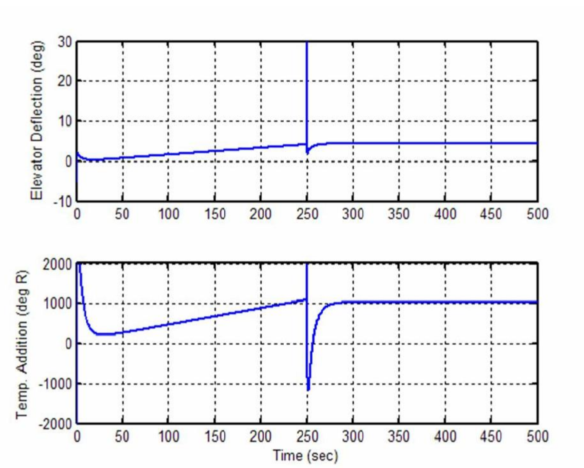

Figure 6. Control Deflections vs. Time - Case 2.

References

[1] M. Bolender and D. Doman,"A Non-Linear Model for the Longitudinal Dynamics of a Hypersonic Airbreathing Vehicle", *Proceedings of the 2005 Guidance, Navigation and Control Conference*, AIAA 2005-6255, August 2005.

[2] M. Oppenheimer and D. Doman, "Reconfigurable Inner Loop Control of a Space Maneuvering Vehicle", *Proceedings of the 2003 Guidance, Navigation and Control Conference*, AIAA 2003-5358, August 2003.

[3] A. Snell, "Decoupling of Nonminimum Phase Plants and Application to Flight Control", *Proceedings of the 2002 Guidance, Navigation and Control Conference*, AIAA 2002-4760, August 2002.

Michael Oppenheimer *Michael W. Oppenheimer is an Electronics Engineer at the Control Design and Analysis Branch at the Air Force Research Laboratory, Wright Patterson Air Force Base, OH. He is the author or co-author of more than 25 publications including refereed conference papers, journal articles, and a technical report. He holds a Ph. D. degree in Electrical Engineering from the Air Force Institute of Technology and is a member of IEEE and AIAA. Dr. Oppenheimer's research interests are in the areas of nonlinear and adaptive control, including reconfigurable flight control and control allocation, and the application of this technology to air vehicles.*

David Doman *David B. Doman is a Senior Aerospace Engineer at the Control Design and Analysis Branch at the Air Force Research Laboratory at Wright Patterson AFB, OH. He is the Technical Area Leader for the Space Access and Hypersonic Vehicle Guidance and Control Team at AFRL. He is the author or co-author of more than 50 publications including, refereed conference papers, journal articles, technical reports and holds one US patent. He holds a Ph.D. degree in Aerospace Engineering from Virginia Tech and is currently an Associate Editor for the Journal of Guidance, Control and Dynamics, a member of the AIAA Guidance, Navigation and Control Technical Committee, an Associate Fellow of the AIAA and a Member of IEEE.*